

## Transport critical current in $c$ -axis-oriented $\text{Bi}_{1.8}\text{Pb}_{0.4}\text{Sr}_2\text{Ca}_2\text{Cu}_3\text{O}_y$ /Ag tapes

G. C. Han\*

*High Magnetic Field Laboratory, Institute of Plasma Physics, Academia Sinica,  
P.O. Box 1126, Hefei 230031, People's Republic of China*

(Received 17 January 1995; revised manuscript received 14 March 1995)

The transport critical current density  $J_c$  of  $c$ -axis-oriented Bi-based silver sheathed tapes was studied as a function of temperature  $T$  and magnetic field  $\mathbf{H}$  in the case of the field applied parallel ( $\mathbf{H}\parallel ab$ ) and perpendicular ( $\mathbf{H}\parallel c$ ) to the tape surface. It can be concluded that the  $J_c$  dependences of the temperature  $J_c(T)$  at various magnetic fields are dominated by the weak-link effect at temperatures very close to  $T_c$  (above 90 K). For the temperatures well below  $T_c$  (77–90 K),  $J_c(T)$  is primarily controlled by the conventional flux creep model of Anderson-Kim in the low-magnetic-field regime. This observation was further confirmed by the field dependence of  $J_c$ . The anisotropy in  $J_c$  can be well described by using the effective-mass model and the overall  $J_c$  of the tapes is determined by the small-angle grain boundaries. In the high-field range, an exponential behavior of  $J_c(\mathbf{H})$  at higher temperatures and a linear  $J_c(\mathbf{H})$  dependence at lower temperatures were clearly observed and can be well accounted for on the basis of collective pinning theory and a strong intrinsic pinning effect, respectively, in this anisotropic material.

### I. INTRODUCTION

The large-scale application of high- $T_c$  superconductivity depends on successful production of long wires with high current-carrying capability. Recently great progress has been made in the fabrication of  $\text{Bi}_2\text{Sr}_2\text{Ca}_2\text{Cu}_3\text{O}_y$  [Bi(2223)] tapes via a powder-in-tube process. High transport critical current densities  $J_c$  exceeding  $6 \times 10^4$  A/cm<sup>2</sup> at 77 K and zero magnetic field have been reported.<sup>1,2</sup> Many theoretical as well as experimental investigations have been carried out<sup>3–8</sup> in order to clarify the limiting factors of the transport  $J_c$ . Starting from the weak grain boundaries, Bulaevskii *et al.*<sup>3</sup> have proposed a so-called “brick wall” model to describe the current transport in polycrystalline Bi-based tapes. They assumed that the grain boundaries along the length of the tape are the essential barriers for transport currents and  $J_c$  is determined by the Josephson currents across the boundaries perpendicular to the tapes. In this approach, the meanderlike current has to flow parallel to the  $c$  axis of the grains and across  $c$ -axis twist boundaries, thus resulting in an overall  $J_c$  behavior similar to the critical current along the  $c$  axis. However, Hensel *et al.*<sup>8</sup> argued that the currents are primarily carried by a small fraction of “strong” grain boundaries along the length of the tape. In this “railway switches” model, the transport  $J_c$  is controlled by the large-area small-angle boundaries. A similar conclusion was also obtained by Tkaczyk *et al.*<sup>6</sup> for  $J_c$  at low temperatures. However, at high temperatures, both Tkaczyk *et al.*<sup>6</sup> and Shibutani *et al.*<sup>9</sup> have suggested that the low  $J_c$  and the dissipations resulted from vortex motion in the well-connected grains. In attempts to explore the  $J_c$ -limiting factors, the  $J_c$  dependence on the field and temperature,  $J_c(H, T)$ , is essential to characterize the samples. In a “brick wall” model, the overall  $J_c(T)$  of the tapes measured with the current along the tape surface is determined by the temperature dependence of the critical current density in the  $c$  direction,

$J_{c,c}(T)$ . On the other hand, Hensel *et al.*,<sup>8</sup> based on their experimental results for  $J_c(T)$  at zero field, showed that  $J_c(T)$  has the same characteristic as the critical current in the  $ab$  plane. Based on the “railway switches” model, the field dependence of the critical current is controlled by the field component along the  $c$  axis, leading to the commonly observed exponential decrease of  $J_c$  with the field. However, at very low fields, a different  $J_c(H)$  behavior is also clearly found, which is generally attributed to the effect of weak grain boundaries. In order to provide a more complete picture of the complex behaviors of  $J_c(H, T)$ , we present our investigations on  $J_c(H, T)$  in more detail.

### II. EXPERIMENT

Samples with the nominal composition  $\text{Bi}_{1.8}\text{Pb}_{0.4}\text{Sr}_2\text{Ca}_2\text{Cu}_3\text{O}_y$  were fabricated by a physical deposition method following the powder-in-tube technique. The precursor powder with fine grains was obtained via nitric acid decomposition from appropriate proportions of high-purity  $\text{Bi}_2\text{O}_3$ ,  $\text{PbO}$ ,  $\text{SrCO}_3$ ,  $\text{CaCO}_3$ , and  $\text{CuO}$  powders and by heat treatment at 800 °C in air for 24 h. The powder was then ground and refined in alcohol, and deposited on a piece of pretreated silver, dried, and pressed at 300 MPa. Then it was put into a silver sheath and pressed at 1200 MPa, forming a silver-sheathed tape. The sample was finally heat treated once at 836 °C in flowing  $\text{O}_2/\text{N}_2$  (1/19) and twice at 845 °C in air with intermediate cold pressing at 2400 MPa. The Ag-sheathed samples (length 15 mm, width 5 mm) had an overall thickness of 80  $\mu\text{m}$  with an oxide core of 40–50  $\mu\text{m}$ . More details of the preparation process were reported elsewhere.<sup>10</sup> The x-ray-diffraction pattern<sup>10</sup> showed that the superconductor was composed of a high- $T_c$  (2223) phase and had a preferential grain orientation with the  $c$  axis perpendicular to the plane of the tape. A scanning electron microscope (SEM) photograph (shown in

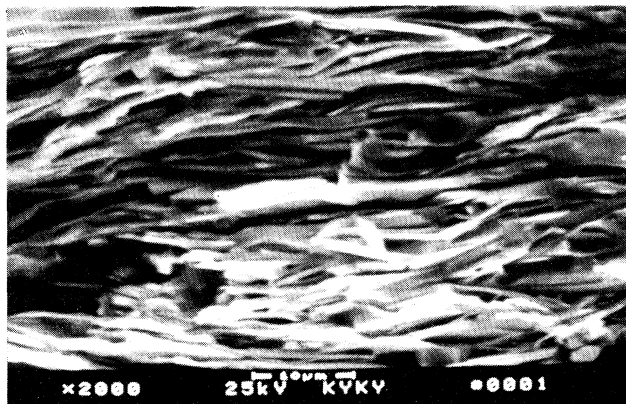


FIG. 1. SEM photograph of the transverse surface of a Bi(2223)/Ag tape with  $J_c(77\text{ K}, 0\text{ T}) = 2.3 \times 10^4\text{ A/cm}^2$ .

Fig. 1) indicated that the sample was well textured, having sharp edges of the grains, which is very similar to the structure observed by Hensel *et al.*<sup>8</sup> Transport  $J_c$  measurements were carried out by a pulsed current method using the dc four-probe technique. For the  $J_c$  determination of the tapes, the standard criterion of  $1\text{ }\mu\text{V/cm}$  was used. The magnetic field was applied perpendicular ( $\mathbf{H}\parallel c$ ) and parallel ( $\mathbf{H}\parallel ab$ ) to the tape surface and always perpendicular to the current direction. The temperature was measured with a calibrated copper-Constantan thermocouple (above  $77\text{ K}$  and at low fields) and a carbon-glass resistor (below  $77\text{ K}$  and at high fields). The sample used in this study has a critical current density  $J_c$  of  $2.3 \times 10^4\text{ A/cm}^2$  at  $77\text{ K}$  and  $0\text{ T}$  unless otherwise mentioned.

### III. RESULTS

#### A. Temperature dependence of critical current density $J_c(T)$

In oxide polycrystalline samples, the temperature dependence of the critical current close to  $T_c$  is usually used to obtain information about the nature of the grain boundaries. It has been reported that the critical currents in polycrystalline samples<sup>11–13</sup> follow the power-law variation  $J_c \propto (1 - T/T_c)^n$  near  $T_c$ , where  $n = 1.5 - 3.5$ . Different types of grain boundaries will give a different value of the exponential factor  $n$ ; for example, if the grain boundaries form superconductor-normal-superconductor (SNS) proximity-effect junctions, one would expect  $n = 2$ ,<sup>14</sup> but for an insulating boundary layer, the calculations by Ambegaokar and Baratoff<sup>15</sup> give  $n = 1$ . Detailed examinations of  $J_c(T)$  for various high- $J_c$  tapes were reported in our previous work.<sup>16</sup> The results indicated that  $J_c$  varied with temperature following a  $(1 - T/T_c)^{3/2}$  functional relationship at zero magnetic field for the samples with  $J_c(77\text{ K}, 0\text{ T}) > 2.0 \times 10^4\text{ A/cm}^2$ . To see the effect of a magnetic field on  $J_c(T)$  characteristics, we have measured  $J_c(T)$  curves in the vicinity of  $T_c$  at various low magnetic fields. Figure 2 gives the  $J_c(T)$  curves in the case of  $\mathbf{H}\parallel ab$ , the solid lines being

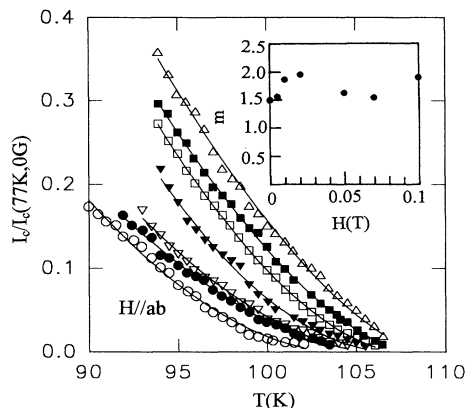


FIG. 2. Temperature dependences of the critical current density for the Bi(2223)/Ag tape near  $T_c$  at several magnetic fields applied parallel to the tape surface ( $\mathbf{H}\parallel ab$ ), displaying a  $J_c \propto (1 - T/T_c)^m$  functional relationship. The inset shows the field dependence of the  $m$  values. The curves correspond to the fields, from top to bottom, 0, 50, 100, 200, 500, 700, and 1000 G.

the fitted curves to the power-law variation  $J_c = A(1 - T/T_c)^m$ , where  $T_c$  was selected as the temperature above which  $J_c$  is below  $5\text{ A/cm}^2$  and thus was dependent on the field. One can see that all the experimental data can be well fitted to the power law. In the fitting process, we used  $m$  and  $A$  as the fitting parameters and fixed the  $T_c$  value, which was determined from the detailed  $J_c(T)$  measurements. By the fitting, the exponential factors can be obtained as functions of the field (shown in the inset of Fig. 2). At zero magnetic field, an exponent of  $m = \frac{3}{2}$  is once again found, but with a magnetic field the  $m$  value changes randomly from 1.5 to 2.0.

For the magnetic field applied parallel to the  $c$  axis ( $\mathbf{H}\parallel c$ ), a linear temperature dependence of  $J_c$  was clearly observed in a wide temperature regime. In Fig. 3, we give an example of  $J_c(T)$  measured for  $\mathbf{H}\parallel c$  at 1000 G. It

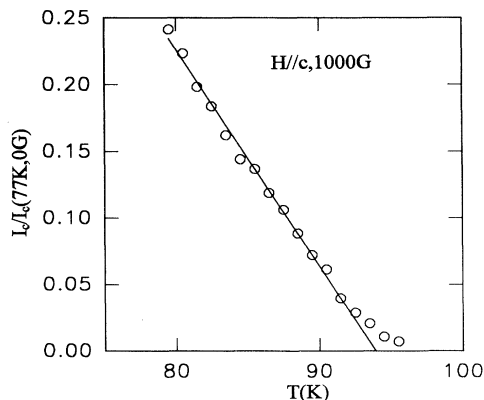


FIG. 3. Temperature dependence of the critical current density for the Bi(2223)/Ag tape for the field applied perpendicular to the tape plane ( $\mathbf{H}\parallel c$ ).

can be seen that  $J_c$  decreases linearly with the increase of temperature, except near  $T_c$ . This linear  $J_c(T)$  dependence was also observed for  $\mathbf{H}\parallel ab$ <sup>17</sup> in the low-temperature range. This characteristic is evidently different from the temperature dependence of the critical current along the *c* axis  $J_{c,c}$  in a Bi(2212) single crystal,<sup>18</sup> implying that in the present Ag-sheathed tapes  $J_c(T)$  is not determined by the  $J_{c,c}$  in the individual grains. This observation clearly demonstrates that the “brick wall” model is invalid to account for  $J_c$  characteristics at least for our samples. We think that the  $J_c$ -limiting mechanism in polycrystalline Bi(2223) tapes is determined mainly by the competition between the weak-link effect and flux motion. At temperatures near  $T_c$ , the Josephson coupling energy is so small that the critical current limited by the grain boundaries is smaller than that governed by the flux motion in the grains. The overall  $J_c$  is thus controlled by the granularity of the samples. As the temperature decreases, the coupling of the grain boundaries becomes stronger and stronger. As a result,  $J_c$  is dominated by the flux motion in the low-temperature regime. From the flux creep theory of Anderson and Kim,<sup>19</sup>  $J_c$  follows:

$$J_c = J_{c0} [1 + kT/U \ln(E_c/a_0 B \Omega)] , \quad (1)$$

where  $J_{c0}$  is the critical current density in the absence of flux creep,  $B$  is the magnetic induction,  $U$  is the activation energy,  $a_0$  is the spacing between pinning centers,  $\Omega$  is the attempt frequency, and  $E_c$  is the voltage criterion for  $J_c$  determination. From Eq. (1), a linear  $J_c(T)$  is clearly predicted, which is consistent with our experimental results in Fig. 3.

### B. Magnetic-field dependence of critical current density $J_c(H)$

The sharp drop of  $J_c$  in the low-magnetic-field regime is commonly attributed to the weakly coupled grain boundaries. A typical effect of the weak links is the appearance of irreversible  $J_c(H)$  dependence at low magnetic fields.<sup>20</sup> The  $J_c(H)$  measurement for increasing and decreasing field, however, showed a reversible field dependence of  $J_c$  (not given in this paper). Therefore other methodologies to analyze the  $J_c$ -limiting mechanism should be applied. First of all, let us examine the general picture of  $J_c(H)$  for  $\mathbf{H}\parallel c$  and  $\mathbf{H}\parallel ab$  at various temperatures. According to the effective-mass model proposed by Hao and Clem,<sup>21</sup> for an anisotropic superconductor the critical current density  $J_c$  as a function of the field and the angle  $\theta$  between  $\mathbf{H}$  and the *c* axis is governed by the reduced field  $h$ , i.e.,

$$J_c(H, \theta) = J_c(h) , \quad (2)$$

where  $h = H(\sin^2\theta/\gamma^2 + \cos^2\theta)^{1/2}$  and  $\gamma = (m_c/m_{ab})^{1/2}$  is the anisotropy factor. In the cases of both  $\mathbf{H}\parallel c$  and  $\mathbf{H}\parallel ab$ , we have

$$h = H/\gamma . \quad (3)$$

Thus Eq. (2) provides a simple scaling form:

$$J_c^{\parallel c}(H) = J_c^{\parallel ab}(\gamma H) . \quad (4)$$

Equation (4) suggests that the  $J_c$  value at a field  $H$  for  $\mathbf{H}\parallel c$  is equal to that at a field  $\gamma H$  for  $\mathbf{H}\parallel ab$ .

To examine this scaling form, in Fig. 4 we show the  $J_c(H)$  curves for  $\mathbf{H}\parallel c$  by solid lines for various temperatures. Experimental data for  $\mathbf{H}\parallel ab$  are given by fitting the data to the corresponding  $J_c^{\parallel c}(H)$  curves using  $\gamma$  as the fitting parameter through Eq. (4). The fitted data are plotted by symbols in Fig. 4. It is evident that the experimental results for  $\mathbf{H}\parallel c$  and  $\mathbf{H}\parallel ab$  can be well described by the effective-mass model through the scaling form of Eq. (4). However, it should also be pointed out that the  $\gamma$  values obtained from the fitting are only around 4, which is much smaller than the value 17–20 obtained from magnetization measurements.<sup>22</sup> In addition,  $\gamma$  was found to decrease slightly with increase of temperature, which is consistent with the result obtained from dissipation measurements.<sup>23</sup> The smaller  $\gamma$  value in the present measurement is evidently not intrinsic because Eq. (3) may be invalid due to the existence of the small-angle grain boundaries (see Fig. 1). As discussed in Ref. 8, because of the strong anisotropy in Bi(2223) superconductors with respect to the orientation in the applied magnetic field, misalignment angles of only a few degrees from the “ideal” direction ( $\mathbf{B}\perp\mathbf{J}$ ,  $\mathbf{B}\parallel ab$ ,  $\mathbf{J}\parallel ab$ ) will induce a steep decrease of critical current. Using  $\gamma=20$  and  $H/h=4$  from the fitting, one can obtain the angle  $\theta=85^\circ$ , which means that on the average there is a  $5^\circ$  misalignment from the *ab* plane for the small-angle grain boundaries in the present sample. To get a deeper insight into the nature of the  $J_c$  characteristics, it is fundamental to explore the functional form of  $J_c(H)$ . Up to now, there have been many forms proposed to account for the  $J_c(H)$  curves. The power-law and exponential dependences of  $J_c(H)$  are two of the most important and often observed experimentally. As pointed out by Dew-Hughes,<sup>24</sup> in the case of  $\Delta W \ll kT$ , where  $\Delta W$  is the work done by the imposed stress in moving flux lines (or bundles), we have

$$J_c(H) = (E_c N_p kT / 2.3 \Phi_0 \Omega B) \exp(U/kT) , \quad (5)$$

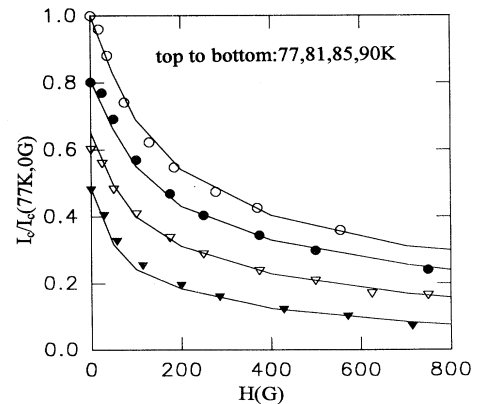


FIG. 4. A scaling plot of  $J_c(H)$  curves for  $\mathbf{H}\parallel c$  and  $\mathbf{H}\parallel ab$  using  $J_c^{\parallel c}(H) = j_c^{\parallel ab}(H/\gamma)$ . The solid lines give the true experimental results for  $\mathbf{H}\parallel c$ . The symbols show the experimental results of  $J_c(H)$  for  $\mathbf{H}\parallel ab$  fitted to those for  $\mathbf{H}\parallel c$  using the scaling form.

where  $N_p$  is the density of the pinning centers and  $\Phi_0$  is the flux quantum. Equation (5) predicts an apparent power-law function of  $J_c(H)$ . This power-law variation was also found with  $J_c(H) \propto H^{-1/2}$  in a melt-processed Y-based oxide superconductor<sup>25</sup> and with  $J_c(H) \propto H^{-n}$  for polycrystalline samples.<sup>26</sup> Anyway, one can expect a linear dependence in the log-log plot of  $J_c(H)$ . The exponential  $H$  dependence is predicted from collective pinning theory.<sup>27</sup> This exponential  $H$  dependence of critical current was observed by several authors.<sup>29,28,9,6</sup> However, for our experimental data, neither of these  $J_c(H)$  functional relationships can be found; instead, a logarithmic field dependence of  $J_c$ , i.e.,  $J_c \propto \ln(H)$ , was clearly observed for  $\mathbf{H}||c$  and  $\mathbf{H}||ab$  in the low-field regime at several temperatures above 77 K. In Fig. 5 the  $J_c(H)$  data are given in a semilogarithmic plot. From Figs. 5(a) and 5(b), one can see that all isothermal  $J_c(H)$  data follow a logarithmic functional relationship within the tolerable experimental errors. This  $J_c(H)$  behavior can be interpreted using Anderson and Kim's flux creep theory. If small effects due to the field dependence of  $J_{c0}$  and  $U$  are neglected in the low-field regime, using  $a_0 = 1.07(\Phi_0/B)^{1/2}$  the logarithmic  $H$  dependence of  $J_c$ , i.e.,  $J_c \propto \ln(H)$ , is apparent from Eq. (1). Thus, we have shown that both  $J_c(H)$  and  $J_c(T)$  can be consistently expressed through

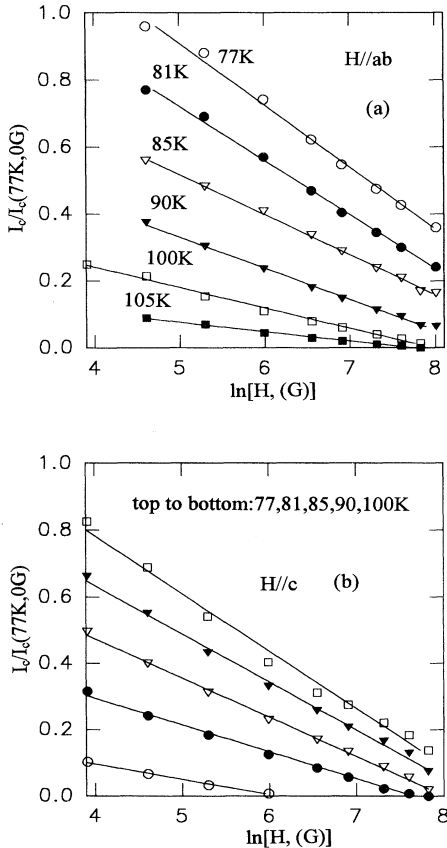


FIG. 5. Magnetic-field dependences of the critical current at various temperatures (a)  $\mathbf{H}||ab$  and (b)  $\mathbf{H}||c$ .

the flux creep model<sup>19</sup> at low magnetic fields.

In the high-magnetic-field regime, different  $J_c(H)$  characteristics were also observed. Figure 6 illustrates the  $J_c(H)$  curves ( $\mathbf{H}||ab$ ) for two different samples with  $J_c(77\text{ K}, 0\text{ T}) = 1.8 \times 10^4\text{ A/cm}^2$  (filled circles) and  $1.5 \times 10^4\text{ A/cm}^2$  (open circles). One can see clearly that  $J_c(H)$  of both samples follows an exponential law with a slightly steeper variation for the lower- $J_c$  sample. This result is in agreement with those commonly observed<sup>28,29,6,9</sup> and can be interpreted from collective pinning theory.<sup>27</sup> We think that, because the interaction energy between flux lines is very weak in the low-field range, the individual flux pinning within the superconducting grains is dominant in the process of flux motion. As a result, Anderson and Kim's flux creep model can be applied. However, in the high-field regime the flux lines are strongly overlapping, resulting in a stronger interaction energy between flux lines, which stabilizes the flux lattice. In this case, an individual pinning center can cause only a weak deformation of the flux line lattice. When a current is applied, a large region of the flux line lattice containing many pinning centers displaces as a whole, thus resulting in a collective pinning effect. At low temperatures (e.g., below 77 K) and high magnetic fields, a linear  $J_c(H)$  dependence was found in some field and temperature ranges depending on the sample's details, shown in Fig. 7 and Figs. 5 and 6 of Ref. 10. In our opinion, the strong intrinsic flux pinning in Bi-based superconductors must be responsible for this  $J_c(H)$  behavior. As proposed by Tachiki and Takahashi<sup>30</sup> for Y-based oxide superconductors, the maximum pinning force density  $F_{PM}$  has the form:

$$F_{PM} \propto B/B_0(1 - B/H_{c2}), \quad (6)$$

where  $H_{c2}$  is the upper critical field along the  $c$  axis and  $B_0$  is a reduced constant. Thus  $J_c$  can be derived from  $F_{PM} = J_c \times B$ , i.e.,

$$J_c = J_c(T)(1 - B/H_{c2}), \quad (7)$$

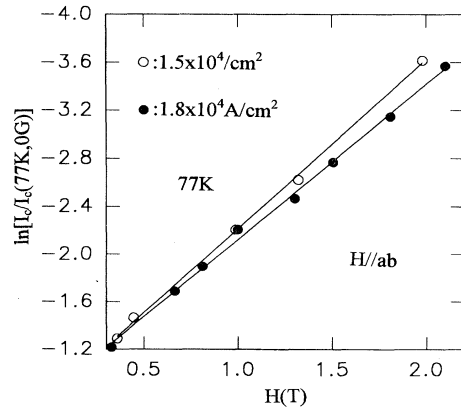


FIG. 6. Magnetic-field dependences of the critical current at 77 K for two Bi(2223)/Ag samples with  $J_c(77\text{ K}, 0\text{ T}) = 1.8 \times 10^4$  and  $1.5 \times 10^4\text{ A/cm}^2$ , showing the exponential dependence of  $J_c(H)$ .

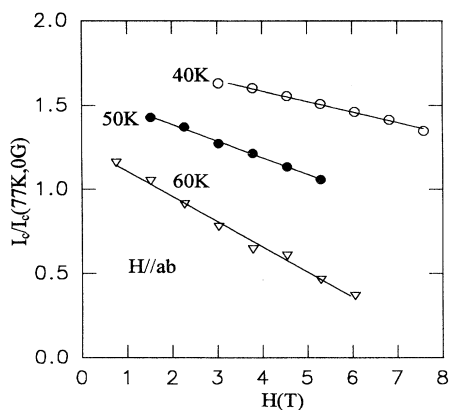


FIG. 7. Magnetic-field dependences of the critical current for two Bi(2223)/Ag tapes at several low temperatures, indicating the linear dependence of  $J_c(H)$  in some temperature and field regimes.

where  $J_c(T)$  is a field-independent function of temperature. Equation (8) clearly predicts a linear  $J_c(H)$  functional relationship, which is consistent with our experimental observations in the low-temperature and high-field regions.

#### IV. CONCLUSION

The detailed studies of  $J_c(H, T)$  characteristics were carried out to clarify the  $J_c$ -limiting mechanism in *c*-axis-oriented Bi(2223)/Ag tapes. From the experimental results, the following can be concluded. (1) At temperatures very close to  $T_c$ ,  $J_c$  is dominated by the granularity of the superconductors. (2) At low magnetic fields and temperatures above 77 K,  $J_c$  is limited by the flux creep. The  $J_c(H, T)$  behaviors seem to support the “railway switches” model if the anisotropic effect in Bi(2222) superconductors is considered. (3) For low temperatures and high magnetic fields, collective pinning and strong intrinsic pinning can be found in different field and temperature regimes, which are dependent on the sample’s details.

#### ACKNOWLEDGMENTS

This work is supported by the National Center of Research and Development on Superconductivity of China under Grant No. J-A-4226. The author would like to thank Dr. S. L. Yuan and Dr. Y. P. Sun for helpful discussion. Thanks are also given to Y. Zhang for his technical assistance in all experimental work and to J. L. Chen, Z. M. Liu, F. T. Wang, W. F. Yuan, and X. N. Liu for their help in high-magnetic-field measurements.

\*FAX: (551) 5591310.

- <sup>1</sup>Y. Yamada, M. Sato, S. Murase, T. Kitamura, and Y. Kamisada, *Advances in Superconductivity* (Springer, Tokyo, 1993), p. 172.
- <sup>2</sup>Q. Li, K. Brodensen, H. A. Hjuler, and T. Freltoft, *Physica C* **217**, 360 (1993).
- <sup>3</sup>L. N. Bulaevskii, J. R. Clem, L. I. Glazman, and A. P. Malozemoff, *Phys. Rev. B* **45**, 2545 (1992).
- <sup>4</sup>M. P. Maley, P. J. Kung, J. Y. Coulter, W. L. Carter, G. N. Riley, and M. E. McHenry, *Phys. Rev. B* **45**, 7566 (1992).
- <sup>5</sup>A. Umezawa, Y. Feng, H. S. Edelman, D. C. Larbalestier, Y. S. Sung, E. E. Hellstrom, and S. Fleshler, *Physica C* **198**, 261 (1992).
- <sup>6</sup>J. E. Tkaczyk, R. H. Arendt, M. F. Garbaskas, H. R. Hart, K. W. Lay, and F. G. Luborsky, *Phys. Rev. B* **45**, 12 506 (1992).
- <sup>7</sup>R. Hergt, R. Hiergeist, J. Taubert, H. W. Neumuller, and G. Ries, *Phys. Rev. B* **47**, 5405 (1993).
- <sup>8</sup>B. Hensel, J.-C. Grivel, A. Jeremie, A. Perin, A. Pollini, and R. Flukiger, *Physica C* **205**, 329 (1993).
- <sup>9</sup>K. Shibusaki, H. J. Wiesmann, R. L. Sabatini, M. Suenaga, S. Hayashi, R. Ogawa, Y. Kawate, L. Motowidlo, and P. Haldar, *Appl. Phys. Lett.* **64**, 924 (1994).
- <sup>10</sup>G. C. Han, H. M. Han, Z. H. Wang, S. X. Wang, F. T. Wang, W. F. Yuan, and J. L. Chen, *Cryogenics* **34**, 613 (1994).
- <sup>11</sup>H. W. Neumuller and G. Ries, *Physica C* **160**, 471 (1989).
- <sup>12</sup>S. X. Dou, H. K. Liu, M. H. Apperley, K. H. Song, and C. C. Sorrell, *Supercond. Sci. Technol.* **3**, 130 (1990).
- <sup>13</sup>H. Masuda, F. Mizuro, I. Hirabashi, and S. Tanaka, *Jpn. J. Appl. Phys.* **28**, L1226 (1989).
- <sup>14</sup>P. G. de Gennes, *Rev. Mod. Phys.* **36**, 225 (1964).
- <sup>15</sup>V. Ambegaokar and A. Baratoff, *Phys. Rev. Lett.* **10**, 486

(1963); **11**, 104 (1963).

- <sup>16</sup>G. C. Han, Y. G. Wang, H. M. Han, Z. H. Wang, S. X. Wang, W. F. Yuan, Q. L. Huang, Z. M. Liu, and J. L. Chen, *Appl. Phys. A* **57**, 363 (1993).
- <sup>17</sup>G. C. Han, H. M. Han, Z. H. Wang, X. L. Liu, Y. F. Yuan, and F. T. Wang, *Phys. Rev. B* **51**, 12 754 (1995).
- <sup>18</sup>R. Kleiner, F. Steinmeyer, G. Kunkel, and P. Muller, *Phys. Rev. Lett.* **68**, 2394 (1992).
- <sup>19</sup>P. W. Anderson and Y. B. Kim, *Rev. Mod. Phys.* **36**, 39 (1964).
- <sup>20</sup>J. E. Evetts and B. A. Glowacki, *Cryogenics* **28**, 641 (1988).
- <sup>21</sup>Z. Hao and J. R. Clem, *Phys. Rev. B* **46**, 5853 (1992).
- <sup>22</sup>Qiang Li, H. J. Wiesmann, M. Suenaga, L. Motowidlow, and P. Haldar, *Phys. Rev. B* (to be published).
- <sup>23</sup>S. L. Yuan, Z. J. Yang, K. Kadowaki, J. Q. Li, T. Kimura, K. Kishio, Z. Huang, J. L. Chen, and B. J. Gao, *Appl. Phys. Lett.* **59**, 583 (1994).
- <sup>24</sup>D. Dew-Hughes, *Cryogenics* **28**, 674 (1988).
- <sup>25</sup>M. Murakami, S. Gotoh, N. Koshizuka, S. Tanaka, T. Matsushita, S. Kambe, and K. Kitazawa, *Cryogenics* **30**, 390 (1990).
- <sup>26</sup>S. X. Wang, Y. G. Wang, S. L. Yuan, and X. Y. Zhou, *Chin. J. Low Temp. Phys.* **14**, 155 (1992); *Dimos et al.*, *Phys. Rev. Lett.* **61**, 219 (1988).
- <sup>27</sup>A. I. Larkin and Yu. N. Ovchinnikov, *J. Low Temp. Phys.* **34**, 409 (1979).
- <sup>28</sup>A. Zhukov *et al.*, *Supercond. Sci. Technol.* **5**, S153 (1992).
- <sup>29</sup>S. Senoussi, M. Oussena, G. Collin, and I. A. Campbell, *Phys. Rev. B* **37**, 9792 (1988).
- <sup>30</sup>M. Tachiki and S. Takahashi, *Solid State Commun.* **70**, 291 (1989).

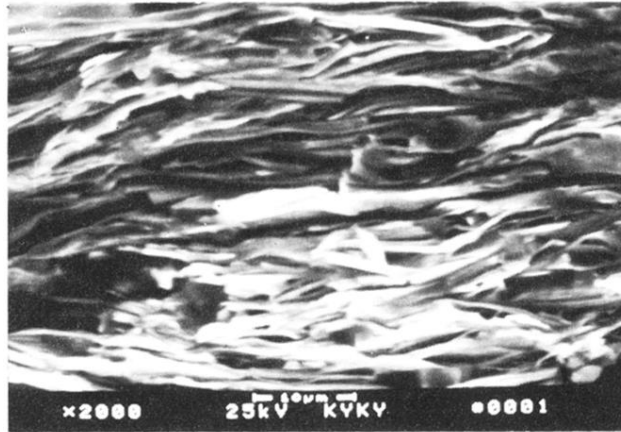


FIG. 1. SEM photograph of the transverse surface of a Bi(2223)/Ag tape with  $J_c(77\text{ K}, 0\text{ T})=2.3 \times 10^4\text{ A/cm}^2$ .